Charge states of atoms in the lattices of the high-temperature superconductors $HgBa_2Ca_{n-1}Cu_nO_{2n+2}$

2000 J. Phys.: Condens. Matter 12 7771

(http://iopscience.iop.org/0953-8984/12/35/312)

J. Phys.: Condens. Matter **12** (2000) 7771–7779. Printed in the UK PII: S0953-8984(00)10735-0

Charge states of atoms in the lattices of the high-temperature superconductors $HgBa_2Ca_{n-1}Cu_nO_{2n+2}$

F S Nasredinov, V F Masterov†, N P Seregin and P P Seregin

St Petersburg State Technical University, 29 Polytekhnicheskaya st., St Petersburg 195251, Russia

Received 4 January 2000

Abstract. Electric field gradient tensor parameters for the copper, barium and mercury sites of the $HgBa_2Ca_{n-1}Cu_nO_{2n+2}$ lattices ($n = 1, 2, 3$) have been determined by the emission Mössbauer spectroscopy on the $^{67}Cu(^{67}Zn)$, $^{133}Ba(^{133}Cs)$ and $^{197}Hg(^{197}Au)$ isotopes and calculated using the point charge approximation. An analysis of the obtained results together with published ^{63}Cu NMR data has shown that an agreement between the experimental and calculated parameters is possible under assumption that holes arising from lattice defects are mainly located in oxygen sublattices of the Cu–O planes (Cu(2)–O plane for $HgBa_2Ca_2Cu_3O_8$).

1. Introduction

The compounds $HgBa_2Ca_{n-1}Cu_nO_{2n+2}$ (HgBaCaCuO) with $n = 1, 2$ and 3 are materials with very high superconducting transition temperature T_c. In this connection, determining the charge state is of particular interest for oxygen atoms believed to be responsible for the phenomenon of high-temperature superconductivity in HgBaCaCuO. These charge states can, in principle, be found by comparing measured and calculated parameters of quadrupole interaction for nuclei at certain lattice sites [1]. In the present work, the emission Mössbauer spectroscopy (EMS) on the $^{67}Cu(^{67}Zn)$, $^{133}Ba(^{133}Cs)$ and $^{197}Hg(^{197}Au)$ isotopes has been used to measure the nuclear quadrupole interaction parameters in HgBaCaCuO lattices.

2. Experimental procedure

HgBaCaCuO ceramic samples were synthesized according to [2–4]. $HgBa_2Ca_{n-1}{}^{67}Cu_nO_{2n+2}$ and $^{197}HgBa_2Ca_{n-1}Cu_nO_{2n+2}$ Mössbauer sources were prepared by diffusion doping of $HgBa_2Ca_2Cu_3O_8$ ((1223), $T_c = 112$ K), $HgBa_2CaCu_2O_6$ ((1212), $T_c = 93$ K) or $HgBa_2CuO_4$ ((1201), $T_c = 79$ K) ceramic samples with the ^{67}Cu and ^{197}Hg radioactive isotopes at 350 °C for 2 hours in an oxygen atmosphere. Conforming with [2–4], annealing of test samples under the same conditions did not lead to any perceptible changes of T_c. The ^{133}Ba radioactive isotope was introduced into the $HgBa_2Ca_{n-1}Cu_nO_{2n+2}$ ceramics during synthesis. $^{67}Cu(^{67}Zn)$ and $^{133}Ba(^{133}Cs)$ Mössbauer spectra were recorded at 4.2 K with ^{67}ZnS and CsCl absorbers, respectively. $^{197}Hg(^{197}Au)$ spectra were taken at 80 K with a metallic gold absorber. Typical spectra are shown in figures 1–3 and the results of their processing are presented in the table 1.

† Deceased.

0953-8984/00/357771+09$30.00

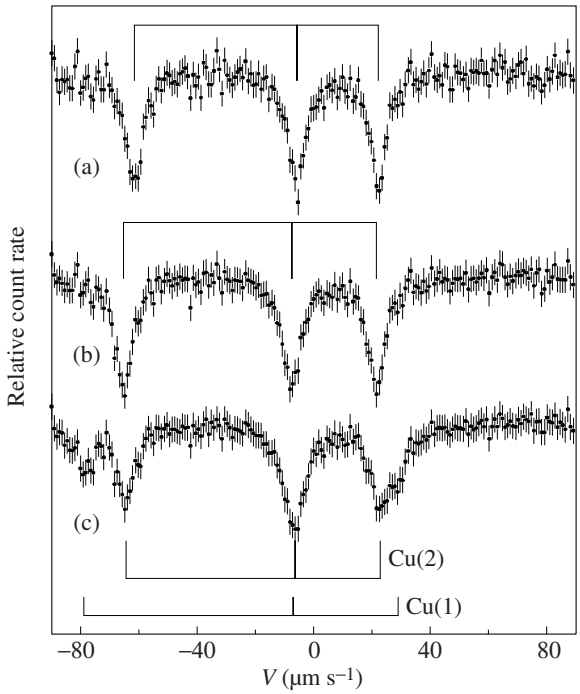

Figure 1. (*a*) ^{67}Cu(^{67}Zn) Mössbauer spectra of (1201), (*b*) (1212) and (*c*) (1223) HgBaCaCuO compounds. Positions of components of the quadrupole triplets corresponding to $^{67}Zn^{2+}$ centres at copper sites are indicated.

Table 1. Parameters of nuclear quadrupole interaction for ^{67}Zn, ^{133}Cs and ^{197}Au probes at cation sites of the $HgBa_2Ca_{n-1}Cu_nO_{2n+2}$ lattices. C are the quadrupole interaction constants (in MHz), η the asymmetry parameter, and V_{zz} the principal component of the lattice EFG, calculated for type A and B models (in e Å^{-3} units).

Compound	Site	Probe	^{67}Zn		^{133}Cs	^{197}Au	V_{zz}	
			C(Zn)	η	|C(Cs)|	|C(Au)|	A	B
$HgBa_2CuO_4$	Cu	^{67}Zn	14.0(5)	$\leqslant 0.2$			0.858	0.737
	Ba	^{133}Cs			$\leqslant 40$		0.080	0.076
	Hg	^{197}Au				262(6)	−1.078	−1.032
$HgBa_2CaCu_2O_6$	Cu	^{67}Zn	14.5(5)	$\leqslant 0.2$			0.937	0.753
	Ba	^{133}Cs			$\leqslant 40$		0.088	0.093
	Hg	^{197}Au				268(6)	−1.100	−0.961
$HgBa_2Ca_2Cu_3O_8$	Cu(1)	^{67}Zn	18.0(5)	$\leqslant 0.2$			1.010	1.006
	Cu(2)	^{67}Zn	14.6(5)	$\leqslant 0.2$			0.931	0.766
	Ba	^{133}Cs			$\leqslant 40$		0.064	0.071
	Hg	^{197}Au				264(6)	−1.138	−1.010

3. Results and discussion

The doping processes were assumed to place the ^{67}Cu, ^{133}Ba and ^{197}Hg parent atoms at copper, barium and mercury lattice sites, respectively. Thus, the ^{67}Zn, ^{133}Cs and ^{197}Au daughter atoms were expected to be found at the same lattice sites. Since all the HgBaCaCuO lattices have only

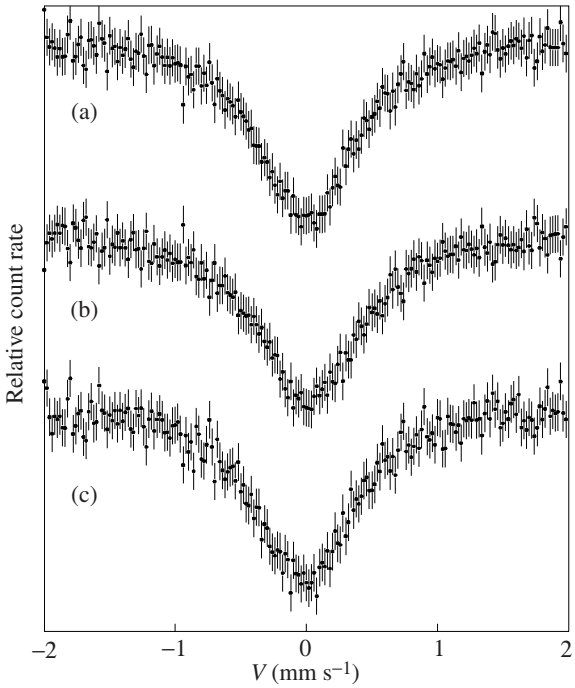

Figure 2. (*a*) ^{133}Ba(^{133}Cs) Mössbauer spectra of (1201), (*b*) (1212) and (*c*) (1223) HgBaCaCuO compounds.

one barium and one mercury positions [5, 6], any ^{133}Ba(^{133}Cs) or ^{197}Hg(^{197}Au) Mössbauer spectrum must reveal only a single state of the respective probe. The spectra in figures 2 and 3 support this conclusion. The (1201) and (1212) compounds have only one copper position [5, 6], too, and their ^{67}Cu(^{67}Zn) spectra correspond to a single state of the ^{67}Zn probe (see figures 1(*a*) and (*b*)). Finally, the (1223) lattice has two different copper positions [6], and the ^{67}Cu(^{67}Zn) Mössbauer spectrum of this compound shows two ^{67}Zn triplets corresponding to the Cu(1) and Cu(2) sites (figure 1(*c*)).

The local symmetry of all lattice sites in the HgBaCaCuO compounds is non-cubic and interaction of the probe's nuclear quadrupole moment eQ with the electric field gradient (EFG) results in a splitting of the Mössbauer spectrum into several components. In the ^{67}Zn case, the experimental spectrum is split into three components, which allows determining the magnitude and sign of the quadrupole interaction constant $C(\mathrm{Zn}) = eQU_{zz}/h$ for the ^{67}Zn probe and the asymmetry parameter η of the EFG tensor.

There exists a correlation between the observed C(Zn) values and the local environment of the Cu–O layers. The C(Zn) value, which is lower for (1201) than for (1212), corresponds to a more symmetric BaO–CuO_2–BaO layer configuration in (1201) as compared with the BaO–CuO_2–Ca one in (1212). The C(Zn) value for Cu(2) in (1223) is very close to that in (1212), because the layer configurations are the same in both cases.

It seems to be commonly accepted now that the EFG can be calculated reliably for rather complex lattices only by *ab initio* quantum methods, for example, by the full-potential linear augmented-plane-wave procedure developed by Blaha P *et al* [7–9] for HTSC's and related compounds. In these works, the EFG was calculated directly from the self-consistent electron charge density by Poisson's equation without using Sternheimer shielding/antishielding

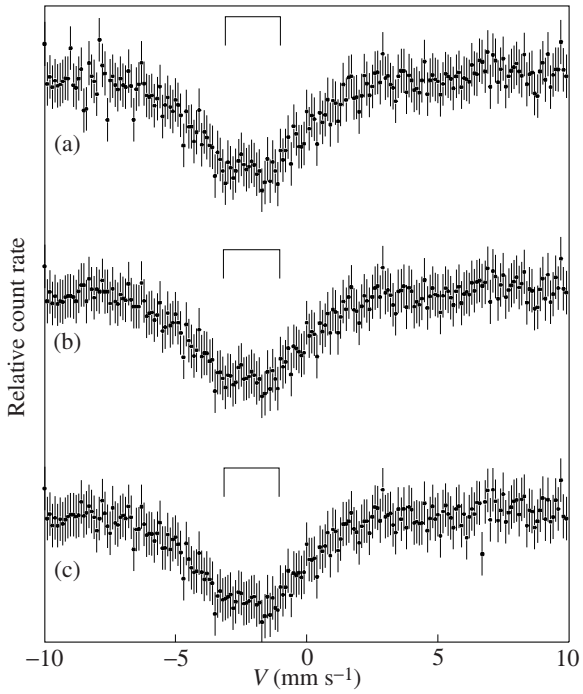

Figure 3. (*a*) ^{197}Hg(^{197}Au) Mössbauer spectra of (1201), (*b*) (1212) and (*c*) (1223) HgBaCaCuO compounds. Positions of components of the quadrupole doublets corresponding to ^{197}Au centres at mercury sites are indicated.

factors. However, this method is rather labour-consuming and hardly suitable for current interpretation of experimental data. Moreover, it cannot be directly employed for calculating the EFG at the impurity probes ^{67}Zn, ^{133}Cs and ^{197}Au used in our case. For these reasons we adhered to a conventional simplified approach and represented the measured eQU_{zz} values as sums of two terms:

$$eQU_{zz} = eQ(1-\gamma_\infty)V_{zz} + eQ(1-R_0)W_{zz} \tag{1}$$

where U_{zz}, V_{zz} and W_{zz} are the principal components of the total, lattice and valence EFG tensors, and γ_∞ and R_0 are the Sternheimer factors for the probe atom.

After the β-decay of the parent ^{67}Cu nucleus, a daughter zinc atom arises in a divalent state that is the only possible valence state of zinc in oxide systems. For the $^{67}Zn^{2+}$ probe, the contribution of the valence electrons into the total EFG tensor can be neglected and equation (1) can be written as

$$C(\mathrm{Zn}) \approx \frac{eQ(1-\gamma_\infty)V_{zz}}{h}. \tag{2}$$

The lattice EFG tensor can be calculated using the point charge model. Its components are calculated as follows:

$$V_{pp} = \sum_k e_k^* \sum_i \frac{1}{r_{ki}^3}\frac{3p_{ki}^2}{r_{ki}^2} - 1$$
$$V_{pq} = \sum_k e_k^* \sum_i \left(\frac{3p_{ki}q_{ki}}{r_{ki}^5}\right)^2 \tag{3}$$

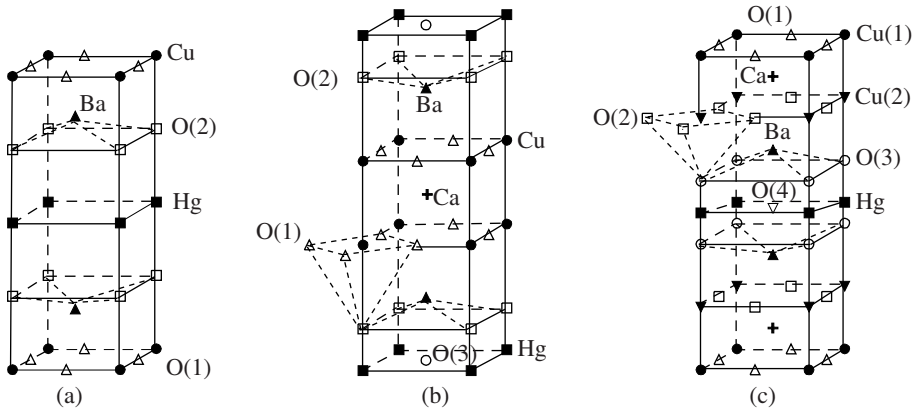

Figure 4. (*a*) Fragments of unit cells of (1201), (*b*) (1212) and (*c*) (1223) lattices.

where k and i are the summing indices for the sublattices and sites within the sublattices, respectively; q and p are the Cartesian coordinates, e_k^* is the charge of atoms of the kth sublattice; and r_{ik} is the distance from the ith site of the kth sublattice to the probe nucleus.

The approximations (1)–(3) require special validation, which was done for ^{67}Cu(^{67}Zn) EMS in a number of HTSC's in our previous works (see, for example, [1, 12]).

The lattice sums have been computed with the summation carried out within a sphere of radius 30 Å (choosing a greater radius of summation did not change the results). According to structural data [5, 6], the lattices can be represented as superpositions of several sublattices:

$$[Hg][Ba_2][Cu][O(1)_2][O(2)_2]\,,$$
$$[Hg][Ba_2][Ca][Cu_2][O(1)_4][O(2)_2]\,,$$
$$[Hg][Ba_2][Ca_2][Cu(1)][Cu(2)_2][O(1)_2][O(2)_4][O(3)_2]\,.$$

The fragments of the HgBaCaCuO unit cells are shown in figure 4. The tensors of contributions from all the sublattices to the EFG proved to be diagonal in the crystal axes and axially symmetric. The results of the calculations are given in table 1 for two models A and B, considered below.

With the standard values $\gamma_\infty = -12.2$ [10] and $Q = 0.17b$ [11] for the $^{67}Zn^{2+}$ probe and the charge distribution model A with conventional valence states of atoms (Hg^{2+}, Ba^{2+}, Ca^{2+}, Cu^{2+}, O^{2-}), the $eQ(1-\gamma_\infty)V_{zz}$ values proved to be 79 MHz and 72 MHz for the Cu(1) and Cu(2) sites of the $HgBa_2Ca_2Cu_3O_8$ lattice, respectively. These values differ essentially from the values C(Zn1) and C(Zn2) measured by the ^{67}Cu(^{67}Zn) EMS (see table 1). This discrepancy may arise from, first, an invalid Sternheimer factor, second, wrong charges of the atoms involved and, third, incorrect use of the point charge model in calculating the EFG for the HgBaCaCuO compounds. The error arising from uncertainty in γ_∞ can be eliminated by comparing the ratios $S = C(\mathrm{Zn1})/C(\mathrm{Zn2}) = 1.23(8)$ and $s = V_{zz1}/V_{zz2} = 1.08$. The difference between S and s is not so large as that between the measured and calculated eQV_{zz} values, which points to an overstated Sternheimer factor for Zn^{2+}, resulting in an overstated $eQ(1-\gamma_\infty)V_{zz}$ value. However, the difference remains rather significant. Similar differences between measured and calculated eQV_{zz} values were also observed for other HgBaCaCuO compounds. The second and third contributions to the differences cannot be separated merely by direct comparison of the measured eQU_{zz} and calculated V_{zz} values.

The origin of these contradictions can be found on the basis of a combined analysis of the ^{67}Cu(^{67}Zn) EMS data and the ^{63}Cu nuclear magnetic resonance (NMR) data for copper

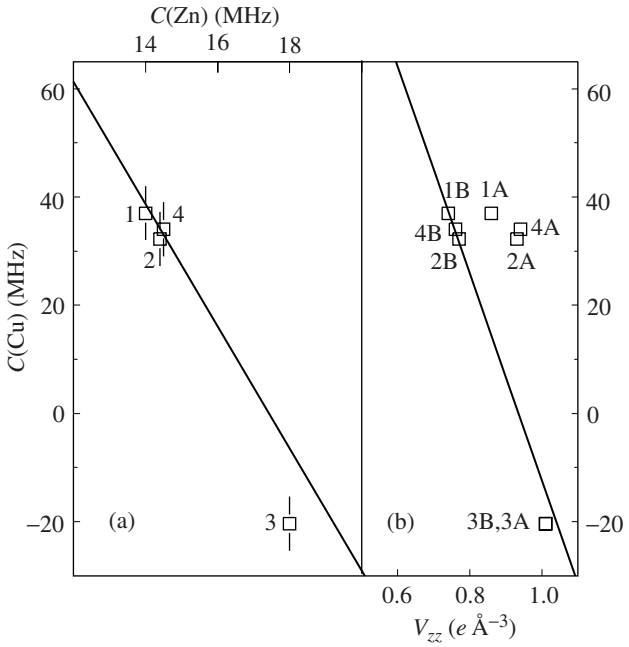

Figure 5. (*a*) C(Cu) versus C(Zn) (full line) and (*b*) C(Cu) versus V_{zz} diagrams for divalent copper compounds. The points represent: 1—Cu in (1201), 2—Cu in (1212), 3—Cu(1) in (1223), 4—Cu(2) in (1223). The symbols A and B designate the models used in the V_{zz} calculations.

sites in various copper oxide compounds. Figure 5(*a*) shows the C(Cu) versus C(Zn) diagram proposed in [12]. For a number of divalent copper compounds, experimental data fall on the straight line

$$C(\mathrm{Cu}) = 197 - 11.3C(\mathrm{Zn}) \tag{4}$$

where both C(Cu) and C(Zn) are given in MHz. This correlation was explained by a nearly constant valence contribution $(1 - R_0)W_{zz}$ to the EFG at copper nuclei, and a non-divalent state of copper was found to be the main reason for deviations from the straight line (4).

^{63}Cu NQR data for the (1201) [13], (1212) [14] and (1223) [15] compounds are plotted in the C(Cu) versus C(Zn) diagram (figure 5(*a*)) together with our ^{67}Cu(^{67}Zn) EMS data. It is seen that all the points are described satisfactorily by equation (4). This means that copper is divalent in HgBaCaCuO compounds.

Some additional information can be extracted from a C(Cu) versus V_{zz} diagram [12] (figure 5(*b*)). On the abscissa axis in this diagram are plotted calculated principal components of the lattice EFG tensors V_{zz} for copper sites in which the C(Cu) values have been measured by the ^{63}Cu NMR. The C(Cu) versus V_{zz} diagram is described by the equation:

$$C(\mathrm{Cu}) = 179 - 191.4V_{zz} \tag{5}$$

where the C(Cu) and V_{zz} values are given in MHz and e Å^{-3} units, respectively. Equation (5) does not require the Sternheimer factor for Cu^{2+} in explicit form, this factor being included in the empirical coefficient of V_{zz}. For the C(Cu) versus V_{zz} diagram, an additional reason for deviation of its points from the straight line (5) was established. This is the EFG tensor calculation becoming invalid because of a wrong choice of the atomic charges.

In the C(Cu) versus V_{zz} diagram, there is no agreement between the HgBaCaCuO points and the linear dependence (5) in the case when the V_{zz} values are calculated under assumption

of standard atomic charges (model A). Obviously, the deviations from the straight line (5) should be explained by the invalidity of the above model. An agreement can be achieved for type B models which require placing holes in the O(1) sublattice for the (1201) and (1212) compounds and in the O(2) sublattice for the (1223) compound. In the investigated compounds, the holes may arise through transition of a part of mercury atoms into the monovalent state. The fraction of monovalent mercury in model B was varied in calculating the lattice EFG, and figure 5(*b*) shows the results obtained for 30, 90 and 80% monovalent mercury in the (1201), (1212) and (1223) lattices, respectively. It is seen that holes in the oxygen sublattice can eliminate the deviations of the C(Cu) versus V_{zz} diagram points from straight line (5). However, it should be noted that the x-ray photoelectron spectroscopy (see, for example, [16]) gives no evidence in favour of the existence of monovalent mercury existence. This may mean that the oxygen sublattice holes arise from structural defects in the materials. The high hole concentrations obtained for the oxygen sublattices in the HgBaCaCuO compounds, especially in (1223), appear to indicate that the concentrations are only approximate. These results show that, in general, holes may appear in the O(1) sublattice for (1201) and (1212) and O(2) for (1223). It should be emphasized that the existence of holes in the corresponding Cu–O layers has already been shown on the basis of structural data [17]. However, the author of [17] interpreted the increase of positive charge in the Cu–O layers as a rise in copper ion charge. Our data evidence that the positive charge resides on oxygen sites of the same layers.

The quadrupole interaction of the ^{197}Au nuclei gives rise to ^{197}Hg(^{197}Au) Mössbauer spectra of two components with a splitting $QS = (1/2)|eQU_{zz}|(1 + \eta^2/3)^{1/2}$. Such experimental spectra do not allow finding the sign of C or determining separately the magnitudes of C and η. In addition, the ^{197}Au Mössbauer spectroscopy gives no way of identifying the charge state of gold atoms from the isomer shift value. However, this identification is possible [18] by analysing simultaneously the isomer shifts (IS) and quadrupole splittings (QS) of ^{197}Au Mössbauer spectra. Figure 6 shows the IS versus QS diagrams for compounds of mono- and trivalent gold. It is seen that the data for HgBaCaCuO are in good agreement with the diagram for trivalent gold. In other words, the daughter ^{197}Au atoms produced in ^{197}Hg decay occupy the mercury sites in the trivalent state.

As the Au^{3+} ion is not a lattice probe, the measured QS values do not provide lattice EFG parameters. However, it can be assumed that $|C(\mathrm{Au})| \approx 2QS$, since all calculations of the lattice EFG tensor for the mercury sites give $\eta = 0$. The $|C(\mathrm{Au})|$ values for all the HgBaCaCuO compounds are very close to one another, which is in agreement with the results obtained in calculating V_{zz} for the mercury sites by type B model.

Obviously, there is a direct relationship between the valence states of parent ^{197}Hg atoms and daughter ^{197}Au ones. $^{197}Au^+$ and $^{197}Au^{2+}$ must arise from $^{197}Hg^+$ and $^{197}Hg^{2+}$, respectively, after electron capture in ^{197}Hg. However, the $^{197}Au^{2+}$ state is unstable and must transform to one of the stable states: Au^+ or Au^{3+}. The final equilibrium between mono- and trivalent gold is governed by the type and concentration of charge carriers in a material. As far as the HgBaCaCuO superconductors have p-type conductivity in normal state, trivalent gold observed in the ^{197}Hg(^{197}Au) emission Mössbauer spectra supports the divalent state of mercury. This is in agreement with the x-ray photoelectron spectroscopy data [16] and evidences existence of uncontrolled defects producing holes localized in the oxygen sublattices of the HgBaCaCuO compounds.

Finally, all the ^{133}Ba(^{133}Cs) Mössbauer spectra are unsplit single lines. It is only possible to roughly estimate the quadrupole interaction constants $|C(\mathrm{Cs})|$ for the ^{133}Cs probe at the Ba sites, rather than finding them exactly. This fact can be explained by small V_{zz} values in accordance with our calculations for the Ba sites of the HgBaCaCuO compounds (see the table 1).

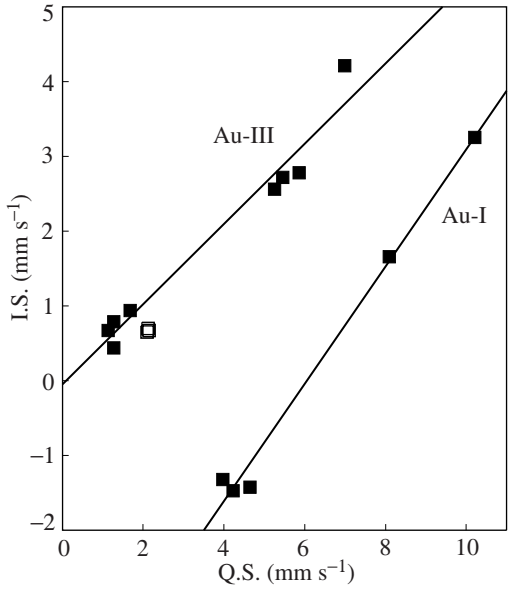

Figure 6. IS versus QS diagrams for mono- and trivalent gold compounds. The experimental data taken from [18] for various gold compounds are represented by full squares. Our data for $HgBa_2CuO_4$, $HgBa_2CaCu_2O_6$ and $HgBa_2Ca_2Cu_3O_8$ are shown by open squares (they coincide practically for all compounds as seen from figure 3). Isomer shifts are given relative to ^{197}Pt metallic source.

4. Conclusion

^{67}Cu(^{67}Zn), ^{133}Ba(^{133}Cs) and ^{197}Hg(^{197}Au) EMS has been used to determine the EFG tensor parameters for the copper, barium and mercury sites of the $HgBa_2Ca_{n-1}Cu_nO_{2n+2}$ lattices. A comparison of the quadrupole interaction constant values for the $^{67}Zn^{2+}$ (the ^{67}Cu(^{67}Zn) EMS data) and $^{63}Cu^{2+}$ (published ^{63}Cu NMR and NQR data) centres with the lattice EFG tensor principal components calculated for the copper sites of the compounds was carried out. Agreement between the measured and calculated parameters of the EFG tensors for the HgBaCaCuO compounds was achieved under assumption that the holes produced by structural defects of the materials are predominantly confined to the oxygen sublattices of the Cu–O planes (in particular, in the Cu(2)–O plane for the (1223) lattice). The ^{133}Ba(^{133}Cs) and ^{197}Hg(^{197}Au) data support these conclusions, too. Being based on the simple point charge model, the above conclusions require further verification.

Acknowledgment

The work was carried out with financial support of the Russian Foundation for Basic Research (grant No 97-02-16216).

References

[1] Jun Chen, Zasadzinski J F, Gray K E, Wagner L L and Hinks D G 1994 *Phys. Rev.* B **49** 3683
[2] Wagner J L, Hunter B A, Hinks D G and Jorgensen J D 1995 *Phys. Rev.* B **51** 15407

[3] Antipov E V, Capponi J J, Chaillout C, Chmaissem O, Loureiro S M, Marezio M, Putilin S N, Santoro A and Tholence J L 1993 *Physica* C **218** 348
[4] Chmaissem O, Wessels L and Sheng Z Z 1994 *Physica* C **230** 231
[5] Wagner J L, Radaelli P G, Hinks D G, Jorgensn J D, Mitchell J F, Dabrowski B, Knapp G S and Beno M A 1993 *Physica* C **210** 447
[6] Finger L W, Hazen R M, Downs R T, Meng R L and Chu C W 1994 *Physica* C **226** 216
[7] Blaha P, Schwarz K and Herzig P 1985 *Phys. Rev. Lett.* **54** 1192
[8] Singh D J, Schwarz K and Blaha P 1992 *Phys. Rev.* B **46** 5849
[9] Ambrosch-Draxl C, Blaha P and Schwarz K 1991 *Phys. Rev.* B **44** 5141
[10] Sternheimer R 1966 *Phys. Rev.* **146** 140
[11] Forster A, Potzel W and Kalvius G M 1980 *Z. Phys.* B **37** 209
[12] Seregin P P, Masterov V F, Nasredinov F S and Seregin N P 1997 *Phys. Status Solidi* b **201** 269
[13] Machi T, Usami R, Yamauchi H, Koshizuka N and Yasuoka H 1994 *Physica* C **235–240** 1675
[14] Horvatic M, Berhier C, Garretta P, Gillet J A, Segransan P, Berthier Y and Capponi J J 1994 *Physica* C **235–240** 1669
[15] Magishi K, Kitaoka Y, Zheng G-q, Asayama K, Tokiwa K, Iyo A and Ihara H 1996 *Phys. Rev.* B **53** R8906
[16] Vasquez R P, Rupp M, Gupta A and Tsuei C C 1995 *Phys. Rev.* B **51** 15657
[17] Shilshtein S Sh 1998 *Phys. Solid State* **40** 1980
[18] Falteus M O and Shirley D A 1973 *J. Chem. Phys.* **59** 5050